HHS Public Access

Author manuscript

ACS Appl Mater Interfaces. Author manuscript; available in PMC 2016 July 21.

Published in final edited form as:

ACS Appl Mater Interfaces. 2016 July 20; 8(28): 17775–17783. doi:10.1021/acsami.6b03245.

Dual-Crosslinked Methacrylated Alginate Sub-Microspheres for Intracellular Chemotherapeutic Delivery

Spencer L. Fenn[#a], **Tianxin Miao**[#a], **Ryan M. Scherrer**[b], and **Rachael A. Oldinski**[a,c,d,*]

[a]Bioengineering Program, College of Engineering and Mathematical Sciences, College of Medicine, University of Vermont, Burlington VT 05405

[b]Department of Microbiology and Molecular Genetics, College of Medicine, University of Vermont Burlington, VT 05405

[c]Mechanical Engineering Program, College of Engineering and Mathematical Sciences, University of Vermont, Burlington, VT 05405

[d]Department of Orthopaedics and Rehabilitation, College of Medicine, University of Vermont, Burlington, VT 05405

[#] These authors contributed equally to this work.

Abstract

Intracellular delivery vehicles comprised of methacrylated alginate (Alg-MA) were developed for the internalization and release of doxorubicin hydrochloride (DOX). Alg-MA was synthesized via an anhydrous reaction, and a mixture of Alg-MA and DOX was formed into sub-microspheres using a water/oil emulsion. Covalently crosslinked sub-microspheres were formed via exposure to green light, in order to investigate effects of crosslinking on drug release and cell internalization, compared to traditional techniques such as ultra violet (UV) light. Crosslinking was performed using light exposure alone, or in combination with ionic crosslinking using calcium chloride ($CaCl_2$). Alg-MA sub-microsphere diameters were between 88 – 617 nm, and zeta-potentials were between −20 and −37 mV. Using human lung epithelial carcinoma cells (A549s) as a model, cellular internalization was confirmed using flow cytometry; different sub-microsphere formulations varied the efficiency of internalization, with UV-crosslinked sub-microspheres achieving the highest internalization percentages. While blank (non-loaded) Alg-MA sub-microspheres were non-cytotoxic to A549s, DOX-loaded sub-microspheres significantly reduced mitochondrial activity after five days of culture. Photo-crosslinked Alg-MA sub-microspheres may be a potential chemotherapeutic delivery system for cancer treatment.

[*]Corresponding Author: Rachael A. Oldinski, 33 Colchester Ave, Votey 201D, Burlington, VT 05405 USA, 802-656-3338, Oldinski@uvm.edu.

Author Contributions

The manuscript was written through contributions of all authors. All authors have given approval to the final version of the manuscript.

SUPPORTING INFORMATION

S1-^{1}H-NMR spectra of Alg-MA and sodium alginate solutions

S2-Scanning electron micrographs of dehydrated Alg-MA sub-microspheres

S3-^{1}H-NMR spectra of doxorubicin hydrochloride solutions exposed to UV and visible green light as compared to unmodified doxorubicin hydrochloride solution.

Keywords

visible light crosslinking; alginate; methacrylation; drug delivery; intracellular; cancer

1. INTRODUCTION

Lung cancer is one of the most widespread type of carcinoma, resulting in the largest number of cancer-related deaths around the world.[1-3] Greater than 85% of lung cancer cases are currently classified as non-small-cell lung cancer (NSCLC), including adenocarcinoma, squamous-cell carcinoma and large-cell carcinoma. Despite the recent advances in early detection and cancer treatment, NSCLC is often diagnosed at an advanced stage and has a poor prognosis.[1] Chemotherapy is one of the current recommended treatments to prevent or reduce tumor-induced symptoms, prolong patient survival, and maintain patient quality of life.[4] Chemotherapy treatments can last as long as 6 months at high parenteral dosages, and are frequently associated with systemic toxicity.[5-6]

Doxorubicin hydrochloride (DOX) is one of the most widely used chemotherapeutic drugs, and is known as an anthracycline antibiotic.[7] The main anti-cancer mechanisms that have been suggested for DOX fall into the following categories: 1) DOX intercalation into DNA, shutting down protein synthesis and DNA replication; 2) DOX-induced production of reactive oxygen species (ROS), inducing DNA damage and/or lipid membrane peroxidation; 3) DNA crosslinking, binding and alkylation; 4) DOX interference with DNA unwinding, strand separation and helicase activity; 5) damage to the bilayer structure of cell membranes; 6) DNA inhibition of topoisomerase II, initiating DNA damage pathways. All the above activities require that DOX be presented inside the cytoplasm,[8-10] which requires intracellular delivery of DOX to cancer cells. DOX treatment induces several side effects including nausea, vomiting, and fever in patients.[11] A significant incidence of cardiovascular side effects – hypotension, tachycardia, arrhythmias, and ultimately congestive heart failure – are also reported.[8, 12] Therefore, there is a need for drug delivery systems which efficiently encapsulate and deliver chemotherapeutics while reducing adverse events. As a small molecule, concerns of low encapsulation efficiency, drug leakage, and aggregation limit the therapeutic efficacy of DOX, and complications associated with sterilization have not been resolved.[5]

Modern drug delivery systems are designed to maintain the structure and bioactivity of biomolecules and to release therapeutics in a controlled and predictable manner. Microencapsulation is one of the core technologies used in polymer drug delivery systems.[13] However, the relatively large micron-size (> 10 μm) of the drug delivery particles limits cellular internalization. Therefore, the association of DOX to sub-micron carriers has drawn greater interest,[14] including liposomes,[15] nanospheres and sub-microspheres,[16] and micelles.[17]

Alginate is an unbranched polysaccharide consisting of 1→4 linked β-D-mannuronic acid (M) and its C-5 epimer α-L-guluronic acid (G). Alginate is extracted from brown seaweed, and has been investigated for biomedical and pharmaceutical applications due to its relatively low cost, low toxicity, biocompatibility, and biodegradability.[18-21] Alginate

particles have increasingly been shown to offer controllable drug encapsulation efficiencies and release profiles, while maintaining the bioactivity of various drugs, including proteins,[22] cytokines,[23] and small molecules.[24] Through the formation of a water/oil emulsion and subsequent exposure to calcium ions, alginate particles within the micrometer – nanometer size scale can be generated, and are often referred to as ionically crosslinked alginate particles.[20, 22, 25]

The fabrication of alginate microspheres and sub-microspheres is favorable for drug delivery due to the relatively mild ionic gelation process.[22, 26] However, limitations associated with the relatively weak ionic bonds include low drug encapsulation efficiency and rapid drug-release rates (< 24 h).[27] To overcome these limitations, methacrylated alginate (Alg-MA) was synthesized [28] and sub-microspheres were generated utilizing a water/oil emulsion [22] and subsequent crosslinking. Alg-MA sub-microspheres were covalently crosslinked using photoinitiators and visible (i.e., green) or UV light irradiation.[28] Dual-crosslinked sub-microspheres were generated with the subsequent addition of calcium chloride.[22] To evaluate the efficiency of internalization and the bioactivity of DOX-loaded Alg-MA sub-microspheres, human lung epithelial carcinoma cells (A549s) were utilized as a model system. We hypothesized the dual-crosslinking would result in a tighter hydrogel network for more efficient intracellular DOX delivery (Figure 1). DOX encapsulation efficiency and *in vitro* release were quantified using an absorbance assay. While blank (non-loaded) Alg-MA sub-microspheres were non-cytotoxic to A549s, DOX-loaded sub-microspheres significantly reduced mitochondrial activity after five days of *in vitro* culture.

2. MATERIALS AND METHODS

2.1. Materials and reagents

Sodium alginate (M_W = 65–75 kg/mol, 60-70% guluronic acid residues) was generously donated by FMC BioPolymer. Irgacure D2959 was generously donated by Ciba Inc. Biology-grade mineral oil, Span 80, Tween 80, ethylenediaminetetriacetic acid (EDTA), deuterium oxide (D_2O), dimethyl sulfoxide (DMSO, 99% anhydrous), dodecyltrimethylammonium bromide salt (DTAB), methacrylic anhydride (MA), 4-(dimethylamino)pyridine (DMAP), DOX, N-ethyl-N'(3-dimethylaminopropyl) carbodiimide hydrochloric acid (EDC), N-hydroxysuccinimide (NHS), and an *in vitro* toxicology assay kit (3-(4,5-dimethylthiazol-2-yl)-2,5-diphenyltetrazolium bromide (MTT)-based) were purchased from Sigma-Aldrich. One molar hydrochloric acid (HCl) and 1 M sodium hydroxide (NaOH) were purchased from BDH ARISTAR®PLUS. Dichloromethane (DCM, 99.9%), sodium citrate, isopropanol, calcium chloride ($CaCl_2$), sodium chloride (NaCl), sodium citrate, Dulbecco's Modified Eagle Medium: Nutrient Mixture F-12 (DMEM/F-12) mammalian cell culture medium, Alexa Fluor® 647 cadaverine and 20X phosphate buffered saline (PBS) were purchased from Fisher Scientific. Fetal bovine serum (FBS) was purchased from Atlanta Biologics. Penicillin, streptomycin, and 0.25% trypsin EDTA were purchased from Corning Cellgro. A549 (CCL-185™) human lung epithelial carcinoma cells were purchased from ATCC®.

2.2. Synthesis and characterization of methacrylated alginate (Alg-MA)

Alg-MA was synthesized utilizing an anhydrous reaction to control the degree of methacrylation (DOM).[28-29] Sodium alginate was rendered soluble in anhydrous DMSO through an ion exchange with DTAB. Aqueous solutions of sodium alginate (1%, w/v) and DTAB (2%, w/v) were prepared and slowly mixed while stirring at 1000 rotations per minute (rpm). The precipitate was washed in DI water and lyophilized. A 1% (w/v) alginate-DTA/DMSO solution was reacted with MA in the presence of a catalyst, DMAP, for 24 hours at room temperature. The solution was hydrolyzed through extensive dialysis in 0.2 M sodium phosphate dibasic salt solution followed by further dialysis in DI water. Alginate methacrylation was confirmed using ^{1}H-NMR spectroscopy, (Bruker AVANCE III 500 MHz high-field NMR spectrometer) by the presence of methacrylate (6.25, 5.75 ppm) and alginate methyl resonances (2.0 ppm). A 1% (w/v) polymer solution in D_2O was analyzed at room temperature, spinning at 20 Hz for 16 scans.[28, 30] The DOM was quantified by peak integration and calculation of the ratio between of the methyl protons at 2.0 ppm and the newly formed methylene protons of methacrylate at 5.75 ppm and 6.25 ppm.[30-31]

2.3. Dual-crosslinked Alg-MA sub-microsphere design and fabrication

2.3.1. Sub-microsphere fabrication—Aqueous Alg-MA solutions were mixed with photoinitiators for UV (0.05%, w/v, Irgacure D2959) or visible green light activation [1 mM eosin Y (photosensitizer), 125 mM triethanolamine (initiator) and 20 mM 1-vinylpyrrolidone (catalyst)], respectively. Two percent (w/v) Alg-MA solutions were mixed with 0.1% (w/v) DOX and formed into sub-microspheres using a water/oil emulsion and subsequent crosslinking (Figure 2). Alg-MA sub-microspheres without DOX were fabricated as blank (i.e., non-loaded) controls.[22] One milliliter of polymer/DOX solution was slowly added to 6.72 mL of biological-grade mineral oil containing 5% (v/v) Span 80, while mixing at 1200 rpm for 5 minutes at room temperature. Subsequently, 400 μL of 30% (v/v) Tween 80 (in biological-grade mineral oil) was added and mixed for an additional 5 minutes. Crosslinking was performed four different ways: 1) green light exposure for 10 minutes (Green, using 525 nm wavelength, NFLS-G30 3-WHT, SuperBrightLEDs); 2) UV light exposure for 10 minutes (UV, using 320–390 nm wavelength, Uvitron Intelliray 400); 3) green light plus 5 mL of 0.5 M $CaCl_2$, mixing for 15 minutes (Green+C); and 4) UV light plus 5 mL of 0.5 M $CaCl_2$, mixing for 15 minutes (UV+C).[28] After crosslinking, 3 mL of isopropanol was added to the emulsion and mixed for 5 minutes, then centrifuged at 400 rpm for 5 minutes to precipitate sub-microspheres. Alg-MA sub-microspheres were washed sequentially with isopropanol (x2) and DI water (x2), respectively, and centrifuged after each wash.

The diameters and zeta-potentials (i.e., surface charge) for hydrated, blank and DOX-loaded Alg-MA sub-microspheres were quantified using dynamic light scattering (DLS, Zetasizer Nano ZSP, Malvern). Sub-microspheres were suspended in PBS, pH = 7.4, at room temperature. Hydrodynamic diameters were determined based on number averages, and the size distribution was plotted for each sub-microsphere group. After lyophilization, Alg-MA sub-microspheres were characterized by scanning electronic microscopy (SEM, JEOL 600); samples were sputter coated with 45 nm of Au-Pb prior to imaging. SEM micrographs of

various magnifications were used to visualize or attempt to visualize Alg-MA sub-microspheres.

2.4. Drug loading and mechanisms of release

Covalently and/or dual-crosslinked Alg-MA sub-microspheres were evaluated for use as chemotherapeutic delivery vehicles. DOX was utilized as a model drug for its intrinsic UV absorbance and ease of quantification, for drug encapsulation, drug release and effectiveness assays. To determine whether or not UV or green light exposure changed the chemical structure or bioactivity of DOX, aqueous DOX solutions were exposed to UV and green light for 10 minutes, and then characterized by ^{1}H-NMR, using non-modified DOX as a control. DOX encapsulation efficiency, i.e., drug retention during sub-microsphere fabrication, was calculated as a percentage of the initial loading concentration. Covalent crosslinking of the sub-microspheres prevents dissolution; therefore, an extended diffusion process was utilized to quantify encapsulated drug. Briefly, 1 mg of sub-microspheres was suspended in 1 mL of PBS, incubated at 37°C and agitated for three weeks. The solution was centrifuged, and the supernatant was analyzed on a microplate reader (Synergy HT microplate reader, BioTek) at 485 nm absorbance, and compared to standard curve (EE = Actual Drug Encapsulated ÷ Theoretical Drug Loaded). Detection of drug lost during washing procedures was not possible due to presence of multiple phases of emulsion additives and the absorbance detection limit of DOX on the equipment utilized.

To characterize *in vitro* release profiles, released DOX concentration was quantified using the intrinsic absorbance at 485 nm in a 48-well tissue culture polystyrene (TCPS) plate at 37°C (Synergy HT microplate reader, BioTek). One milligram of lyophilized DOX-loaded Alg-MA sub-microspheres was dissolved in 500 μL of PBS, pH 7.4 (n = 3). At 1, 2, 4, 8, 12, and 24 hours, and daily up to 11 days, 100 μL of PBS was removed for analysis, and replaced with 100 μL of fresh PBS to maintain the total volume. DOX concentration was determined using an absorbance assay and generating a standard curve. Cumulative DOX (μg) released over time was calculated by adding the mass of DOX released at each time point per mass of sub-microspheres.

2.5. Cellular uptake of Alg-MA sub-microspheres

Four different formulations of blank (i.e., non-loaded) Alg-MA sub-microspheres were reacted with Alexa Fluor® 647 cadaverine dye to form fluorescent sub-microspheres (Alexa 647-Alg-MA); the surface reaction chemistry was performed according to the manufacturers protocol through carbodiimide chemistry at room temperature catalyzed by NHS/EDC. Alg-MA sub-microspheres without DOX were used in order to avoid cell death during internalization and analysis. A549s were seeded in 48-well TCPS plates at 25,000 cells/well in 500 μL/well of standard growth culture medium (DMEM/F-12, 10% FBS, 100 U/mL penicillin, 100 μg/mL streptomycin), and allowed to adhere for 24 hours at 37°C and 5% CO_2. Cells were then incubated with blank Alexa 647-Alg-MA sub-microspheres (n = 6 per group) at 100 μg/mL, 37°C and 5% CO_2. After 12 hours, culture medium containing Alexa 647-Alg-MA submicrospheres was removed, and adherent cells were thoroughly rinsed with PBS three times to remove non-internalized and cell-surface-bound sub-microspheres. Cells were trypsinized and re-suspended in PBS at 1×10^{6} cells/mL, and analyzed by flow

cytometry (BD LSRII Flow Cytometer) to quantify the percentage of A549s that internalized the sub-microspheres. A549s cultured with no sub-microspheres, and cells cultured with non-fluorescent sub-microspheres, were prepared and analyzed as controls.[22]

2.6. Drug bioactivity and efficacy of Alg-MA sub-microsphere delivery vehicles

2.6.1. Cytotoxicity of blank and drug-loaded Alg-MA sub-microspheres—The cytotoxicity of blank (i.e., non-loaded) and DOX-loaded sub-microspheres was evaluated using a toxicology, MTT-based assay. A549s were seeded in 48-well TCPS plates at 25,000 cells/well in 500 μL/well of standard growth culture medium, and allowed to adhere for 24 hours at 37°C and 5% CO_2. Cells were then incubated in the presence of blank Alg-MA sub-microspheres or DOX-loaded Alg-MA sub-microspheres (n = 6 per group, per fabrication type) at sub-microsphere concentrations of 10, 50, 100 μg/mL. After 24 hours, medium containing sub-microspheres (blank groups and DOX-loaded groups) was removed, cells were rinsed two times in sterile PBS, and then analyzed using a MTT-based assay according to the manufacturer's protocol. The optical density was measured at 570 nm; background absorbance at 690 nm was subtracted from the measured absorbance at 570 nm (Synergy HT microplate reader, BioTek). Absorbance values for the experimental samples were normalized to controls and reported as normalized mitochondrial activity.[22]

2.6.2. Effect of intracellular vs. extracellular drug delivery on cell proliferation—The bioactivity of the DOX-loaded sub-microspheres was evaluated using a similar method discussed in section 2.6.1. A549s were seeded in 48-well TCPS plates at 10,000 cells/well in 500 μL/well of standard growth culture medium, and allowed to adhere for 24 hours. Cells were incubated in the presence of DOX-loaded Alg-MA sub-microspheres (n = 6 per fabrication type) at sub-microsphere concentrations of 10, 50, and 100 μg/mL. A549s and Alg-MA sub-microspheres were co-cultured for 5 days with media exchanges. Free DOX (i.e., DOX contained within the cell culture medium) was added to A549s at different concentrations (5, 4, 3, 2, 1, 0.5, 0.25, 0.125, 0.06, 0.03, 0.015 and 0 μg/mL) to compare the effect of intracellular versus extracellular DOX delivery. After 1, 3 and 5 days of culture, a MTT-based assay was performed according to the manufacturer's protocol, to quantify the effects of DOX-loaded Alg-MA sub-microspheres and free DOX on *in vitro* cancer cell proliferation. Absorbance values for the experimental samples were normalized to controls and reported as normalized mitochondrial activity.[22]

2.7. Data analysis

The quantitative results for all experiments are reported as mean ± standard deviation. Statistical analysis was performed on Alg-MA sub-microsphere co-cultured cell assays, using one-way ANOVA with DUNNETs method ($\alpha = 0.05$) via the SAS statistics program in the GLM procedure, as the post-test to compare all of the groups. A $p < 0.05$ was considered significantly different.

3. RESULTS AND DISCUSSION

3.1. Synthesis and characterization of Alg-MA

The chemical modification of alginate rendered it hydrophobic and soluble in organic solvents. An anhydrous methacrylation of alginate resulted in a functionalized biomacromolecule with a controllable DOM.[28] ^{1}H-NMR spectra for Alg-MA and non-modified alginate are shown in Supplemental Figure S1. The DOM for the Alg-MA used as the base material in the sub-microspheres was approximately 64%.[31-34] Peaks between 3.0 and 3.5 ppm indicate methyl groups at the end of alginate chains resulting from degradation during the methacrylation chemistry.

3.2. Fabrication and characterization of dual-crosslinked Alg-MA sub-microspheres

The formation of Alg-MA sub-microspheres was indicative of a crosslinked hydrogel network, obtained through either covalent crosslinking[35] (e.g., via photo-crosslinking) alone, or in combination with ionic crosslinking (e.g., by the addition of $CaCl_2$), as illustrated in Figure 2.[27, 35-36] The DOM for the Alg-MA base material was 64%, and this moderate-DOM sustained both covalent and ionic crosslinking. Photo-crosslinking occurred upon UV or green light activation between adjacent acrylate groups, while the subsequent presence of $CaCl_2$ induced ionic crosslinking between adjacent carboxyl groups. While methacrylation took place at available hydroxyl groups, ionic crosslinks formed between adjacent carboxyl side-groups on neighboring alginate chains, thus allowing Alg-MA to sustain dual-crosslinking.

DOX-loaded sub-microsphere hydrodynamic diameters were quantified using DLS analysis (Table 1). The largest populations of DOX-loaded sub-microspheres were sized between 243 – 391 nm: UV = 243 nm, Green = 391 nm, UV+C = 346 nm, Green+C = 358 nm. The variability of the sub-microsphere diameters, plotted as size distributions in Figure 3A+B, is an almost unavoidable result of the emulsion process, and is indeed a limitation of the fabrication method; however, the linear size distribution plots indicate the following: Alg-MA sub-microspheres exhibited size populations within the same size scale, thus demonstrating consistency in fabrication method. SEM images (see Supplemental Figure S2) also indicated that Alg-MA sub-microspheres were spherical in shape, however heterogeneous in size. The zeta-potentials ranged between −20 mV and −37 mV, and none of the groups demonstrated any significant outlying data.

3.3. Swelling and diffusion-based drug release

The efficacy of Alg-MA sub-microspheres as chemotherapeutic delivery vehicles was investigated. DOX was utilized as a model drug for its intrinsic UV absorbance and ease of quantification for subsequent drug encapsulation, drug release and effectiveness assays. Alg-MA sub-microspheres were designed to encapsulate DOX without interfering with the detectability or bioactivity of DOX. Both photo-crosslinking alone or dual-crosslinking were successful in fabricating DOX-loaded sub-microspheres. The low level of UV or green light exposure required for sub-microsphere fabrication did not change the chemical structure of DOX, verified by ^{1}H-NMR spectroscopy (see Supplemental Figure S3), and the toxic effects of DOX were still active.[37] The mild-gelation techniques used to form Alg-MA sub-

microspheres may retain the functionality and bioactivity of other therapeutics. Indeed, it was hypothesized that secondary, ionic crosslinking may show no beneficial effect on DOX encapsulation efficiency, however, the effect of ionic crosslinking may result in sustained drug release due to a tighter hydrogel network structure.

The cumulative mass of DOX released over time was calculated from four different types of Alg-MA sub-microspheres, and release profiles are shown in Figure 4. The DOX release profiles followed two different trends – a linear release profile was seen during the first 8 hours of release, consistent with hydrogel-swelling induced drug release (see Figure 4A). Cumulative DOX release profiles through 11 days are shown in Figure 4B. The release profiles for UV, Green, and Green+C groups followed a logarithmic trend (trend line $R^2 \geq 0.92$), while the UV+C group followed a linear release profile up to 11 days (trend line $R^2 = 0.98$); however, these trends were not analyzed further. The amount of DOX released did show a similar trend with encapsulation efficiencies: dual-crosslinked sub-microspheres encapsulated less drug and released less drug over an 11 day period.[38-39] The introduction of aqueous-based $CaCl_2$ solution to the emulsion resulted in drug loss due to DOX solubility in aqueous solutions.[40] The varying release kinetics with time suggest that the sub-microsphere structure may be optimized further for controlled release applications, by varying the degree of crosslinking to extend or delay the drug release rate.[35] It is hypothesized that increasing the drug-loading concentration, increased efficacy over longer time periods could be achieved. Decreasing the variability in the diameter of the sub-microspheres and varying the Alg-MA DOM may also result in varied release rates due to changes in the network microstructure. However, sub-microsphere size homogeneity and drug release profile optimization were outside the scope of this study and may be addressed through further investigations.

3.4. Cellular uptake of Alg-MA sub-microspheres

Uptake of Alg-MA sub-microspheres into A549s was quantitatively determined via flow cytometry to detect the fluorescent signal of Alexa-647-labeled sub-microspheres. Non-treated A549s and cells cultured with non-fluorescently labeled sub-microspheres were used as controls. Utilizing gate settings based on the fluorescent intensity level of the probe, negative and positive populations were established, and it was found that all four types of Alg-MA sub-microspheres were readily internalized by A549s.[22] The positive population was > 80% in all four treatment groups (Figure 5A-F). UV crosslinked Alg-MA sub-microspheres (single and dual-crosslinked) exhibited higher internalization rates compared to green light crosslinked groups (Figure 5G), which may be related to sub-microsphere diameter; however, statistics were not performed on the internalization data.

3.5 Cytotoxicity of blank and drug-loaded Alg-MA sub-microspheres

To verify the non-toxicity and retention of DOX bioactivity after sub-microsphere encapsulation, MTT assays were performed on blank Alg-MA sub-microspheres and DOX-loaded Alg-MA sub-microspheres after 24 hours of culture with A549s to quantify mitochondrial activity. A549 viability was assessed in the presence of Alg-MA sub-microspheres at increasing concentrations (10, 50, 100 μg/mL, Figure 6). Blank Alg-MA sub-microspheres (with no drug content) were minimally cytotoxic to A549s (mitochondrial

activity > 80%) at concentrations up to 100 μg/mL (Figure 6A). Increased mitochondrial activity may be attributed to low molecular weight soluble alginate (i.e., sugar) in the culture media. Additionally, we hypothesize the reduced cytotoxicity seen in the UV+C group may be due to enhanced clearance of residual UV photoinitiator upon secondary crosslinking with an aqueous calcium chloride solution.[41] DOX-encapsulated sub-microspheres delivered bioactive drug, significantly reducing mitochondrial activity within 24 hours (Figure 6B).

3.6. Effect of intracellular vs. extracellular drug delivery on cell proliferation

Four different types of DOX-loaded Alg-MA sub-microspheres were cultured with A549s at concentrations of 10, 50 and 100 μg/mL. In addition, different concentrations of free DOX was added to the culture media and served a control. A short-term cell proliferation study (utilizing an MTT assay) was performed for 5 days. On day 1, all of the Alg-MA sub-microsphere groups reduced A549 proliferation, regardless of the crosslinking type or concentration (Figure 7A). On days 3 and 5, the UV crosslinked Alg-MA sub-microspheres showed the greatest reduction in the A549 proliferation. For comparison, normalized mitochondrial activity was plotted versus free DOX, Figure 7B, or DOX-loaded sub-microspheres calculated, Figure 7C. Compared to the free DOX control, Alg-MA sub-microsphere-mediated delivery shows a similar decreasing trend as drug concentration increases, though remains less effective. Also, it is likely that drug remains within the sub-microspheres and is not released intracellularly. Another consideration is that due to the extended drug release profile of DOX from sub-microspheres (Figure 4B), improved efficacy beyond 5 days may be achieved. Indeed, photo-crosslinked microspheres alone are advantageous for delivering a chemotherapeutic to cancer cells, at clinically-relevant dosages, and decreased lung cancer cell mitochondrial activity.

4. Conclusions

The study reported here-in focused on the efficacy of utilizing crosslinked Alg-MA sub-microspheres to intracellularly deliver a chemotherapeutic. Photo-crosslinked and dual-crosslinked Alg-MA sub-microspheres successfully encapsulated DOX, were internalized by A549s, and delivered DOX to A549s, reducing mitochondrial activity compared to non-modified cell controls. The outcome of this study suggests that photo-crosslinking alone, and in particular green light activation, is an effective means of producing drug delivery vehicles, and perhaps additional crosslinking steps or procedures are not beneficial, perhaps even detrimental, to drug encapsulation efficiencies. Based on drug encapsulation predictions and calculations, effective clinical drug dosages were achieved, as compared to free DOX delivery, and were controllable. While the efficacy for using photo-crosslinking Alg-MA sub-microspheres was shown during a short time frame (5 days) *in vitro*, future *in vivo* work may show enhanced drug efficacy using microsphere-mediated delivery compared to exogenous intravenous chemotherapy over extended periods of time.

Supplementary Material

Refer to Web version on PubMed Central for supplementary material.

ACKNOWLEDGMENTS

The authors gratefully acknowledge members of the University of Vermont Microscopy Imaging Center in the College of Medicine for assistance with SEM imaging, and Dr. Roxana del Rio-Guerra for flow cytometry technical work. The authors also express gratitude towards Dr. Appala Raju Badireddy for DLS equipment and assistance, and Jana Vree and Dr. Matt Kinsey for biological expertise and support. This work was supported by the College of Engineering and Mathematical Sciences, and the College of Medicine at the University of Vermont and by NIH training fellowship for Spencer Fenn (T32 HL076122).

REFERENCES

1. Chen Z, Fillmore CM, Hammerman PS, Kim CF, Wong K-K. Non-Small-Cell Lung Cancers: A Heterogeneous Set of Diseases. Nat. Rev. Cancer. 2014; 14(8):535–546. [PubMed: 25056707]
2. Jemal A, Bray F, Center MM, Ferlay J, Ward E, Forman D. Global Cancer Statistics. Ca-Cancer J. Clin. 2011; 61(2):69–90. [PubMed: 21296855]
3. Siegel RL, Miller KD, Jemal A. Cancer Statistics, 2015. Ca-Cancer J. Clin. 2015; 65(1):5–29. [PubMed: 25559415]
4. Manegold C. Chemotherapy for Advanced Non-Small Cell Lung Cancer: Standards. Lung Cancer. 2001; 34(Supplemental 2):S165–170. [PubMed: 11720760]
5. Lee WL, Guo WM, Ho VHB, Saha A, Chong HC, Tan NS, Tan EY, Loo SCJ. Delivery of Doxorubicin and Paclitaxel from Double-Layered Microparticles: The Effects of Layer Thickness and Dual-Drug Vs. Single-Drug Loading. Acta Biomater. 2015; 27:53–65. [PubMed: 26340886]
6. Wong HL, Bendayan R, Rauth AM, Li Y, Wu XY. Chemotherapy with Anticancer Drugs Encapsulated in Solid Lipid Nanoparticles. Adv. Drug Delivery Rev. 2007; 59(6):491–504.
7. Marchal S, Hor AE, Millard M, Gillon V, Bezdetnaya L. Anticancer Drug Delivery: An Update on Clinically Applied Nanotherapeutics. Drugs. 2015; 75(14):1601–1611. [PubMed: 26323338]
8. Carvalho FS, Burgeiro A, Garcia R, Moreno AJ, Carvalho RA, Oliveira PJ. Doxorubicin-Induced Cardiotoxicity: From Bioenergetic Failure and Cell Death to Cardiomyopathy. Med Res Rev. 2014; 34(1):106–135. [PubMed: 23494977]
9. Hortobagyi GN. Anthracyclines in the Treatment of Cancer. An Overview. Drugs. 1997; 54(Supplemental 4):1–7. [PubMed: 9361955]
10. Aubel-Sadron G, Londos-Gagliardi D. Daunorubicin and Doxorubicin, Anthracycline Antibiotics, a Physicochemical and Biological Review. Biochimie. 1984; 66(5):333–352. [PubMed: 6380596]
11. Bonadonna G, Monfardini S, De Lena M, Fossati-Bellani F, Beretta G. Phase I and Preliminary Phase Ii Evaluation of Adriamycin (Nsc 123127). Cancer Res. 1970; 30(10):2572–2582. [PubMed: 5474180]
12. Rochette L, Guenancia C, Gudjoncik A, Hachet O, Zeller M, Cottin Y, Vergely C. Anthracyclines/Trastuzumab: New Aspects of Cardiotoxicity and Molecular Mechanisms. Trends Pharmacol. Sci. 2015; 36(6):326–348. [PubMed: 25895646]
13. Singh MN, Hemant KSY, Ram M, Shivakumar HG. Microencapsulation: A Promising Technique for Controlled Drug Delivery. Res. Pharm. Sci. 2010; 5(2):65–77. [PubMed: 21589795]
14. Janes KA, Fresneau MP, Marazuela A, Fabra A, Alonso M. a. J. Chitosan Nanoparticles as Delivery Systems for Doxorubicin. J. Controlled Release. 2001; 73(2–3):255–267.
15. Li X, Ding L, Xu Y, Wang Y, Ping Q. Targeted Delivery of Doxorubicin Using Stealth Liposomes Modified with Transferrin. Int. J. Pharm. (Amsterdam, Neth.). 2009; 373(1–2):116–123.
16. Couvreur P, Roblot-Treupel L, Poupon MF, Brasseur F, Puisieux F. Nanoparticulate Systems for Drug Delivery Nanoparticles as Microcarriers for Anticancer Drugs. Adv. Drug Delivery Rev. 1990; 5(3):209–230.
17. Hrubý M, Koňák Č, Ulbrich K. Polymeric Micellar Ph-Sensitive Drug Delivery System for Doxorubicin. J. Controlled Release. 2005; 103(1):137–148.
18. Lee KY, Mooney DJ. Alginate: Properties and Biomedical Applications. Prog. Polym. Sci. 2012; 37(1):106–126. [PubMed: 22125349]

19. Wu H, Liao C, Jiao Q, Wang Z, Cheng W, Wan Y. Fabrication of Core–Shell Microspheres Using Alginate and Chitosan–Polycaprolactone for Controlled Release of Vascular Endothelial Growth Factor. React. Funct. Polym. 2012; 72(7):427–437.
20. Baimark Y, Srisuwan Y. Preparation of Alginate Microspheres by Water-in-Oil Emulsion Method for Drug Delivery: Effect of Ca2+ Post-Cross-Linking. Adv. Powder Technol. 2014; 25(5):1541–1546.
21. Miao T, Fenn SL, Charron PN, Oldinski RA. Self-Healing and Thermoresponsive Dual-Cross-Linked Alginate Hydrogels Based on Supramolecular Inclusion Complexes. Biomacromolecules. 2015; 16(12):3740–3750. [PubMed: 26509214]
22. Miao T, Rao KS, Spees JL, Oldinski RA. Osteogenic Differentiation of Human Mesenchymal Stem Cells through Alginate-Graft-Poly(Ethylene Glycol) Microsphere-Mediated Intracellular Growth Factor Delivery. J. Controlled Release. 2014; 192:57–66.
23. Jiang T, Kim YK, Singh B, Kang SK, Choi YJ, Cho CS. Effect of Microencapsulation of Lactobacillus Plantarum 25 into Alginate/Chitosan/Alginate Microcapsules on Viability and Cytokine Induction. J Nanosci Nanotechnol. 2013; 13(8):5291–5295. [PubMed: 23882756]
24. Sosnik A. Alginate Particles as Platform for Drug Delivery by the Oral Route: State-of-the-Art. ISRN Pharm. 2014; 2014:17.
25. Machado AHE, Lundberg D, Ribeiro AJ, Veiga FJ, Lindman B, Miguel MG, Olsson U. Preparation of Calcium Alginate Nanoparticles Using Water-in-Oil (W/O) Nanoemulsions. Langmuir. 2012; 28(9):4131–4141. [PubMed: 22296569]
26. Jay SM, Saltzman WM. Controlled Delivery of Vegf Via Modulation of Alginate Microparticle Ionic Crosslinking. J. Controlled Release. 2009; 134(1):26–34.
27. Tonnesen HH, Karlsen J. Alginate in Drug Delivery Systems. Drug Dev Ind Pharm. 2002; 28(6): 621–630. [PubMed: 12149954]
28. Fenn SL, Oldinski RA. Visible Light Crosslinking of Methacrylated Hyaluronan Hydrogels for Injectable Tissue Repair. J. Biomed. Mater. Res., Part B. 2015 10.1002/jbm.b.33476.
29. Wagner DE, Fenn SL, Bonenfant NR, Marks ER, Borg Z, Saunders P, Oldinski RA, Weiss DJ. Design and Synthesis of an Artificial Pulmonary Pleura for High Throughput Studies in Acellular Human Lungs. Cell Mol Bioeng. 2014; 7(2):184–195. [PubMed: 25750684]
30. Charron PN, Fenn SL, Poniz A, Oldinski RA. Mechanical Properties and Failure Analysis of Visible Light Crosslinked Alginate-Based Tissue Sealants. J. Mech. Behav. Biomed. Mater. 2016; 59:314–321. [PubMed: 26897093]
31. Jeon O, Bouhadir KH, Mansour JM, Alsberg E. Photocrosslinked Alginate Hydrogels with Tunable Biodegradation Rates and Mechanical Properties. Biomaterials. 2009; 30(14):2724–2734. [PubMed: 19201462]
32. Jeon O, Alsberg E. Photofunctionalization of Alginate Hydrogels to Promote Adhesion and Proliferation of Human Mesenchymal Stem Cells. Tissue Eng., Part A. 2013; 19(11-12):1424–1432. [PubMed: 23327676]
33. Jeon O, Alt DS, Ahmed SM, Alsberg E. The Effect of Oxidation on the Degradation of Photocrosslinkable Alginate Hydrogels. Biomaterials. 2012; 33(13):3503–3514. [PubMed: 22336294]
34. Jeon O, Samorezov JE, Alsberg E. Single and Dual Crosslinked Oxidized Methacrylated Alginate/Peg Hydrogels for Bioadhesive Applications. Acta Biomater. 2014; 10(1):47–55. [PubMed: 24035886]
35. Nguyen AH, McKinney J, Miller T, Bongiorno T, McDevitt TC. Gelatin Methacrylate Microspheres for Controlled Growth Factor Release. Acta Biomater. 2015; 13:101–110. [PubMed: 25463489]
36. Hamidi M, Azadi A, Rafiei P. Hydrogel Nanoparticles in Drug Delivery. Adv. Drug Delivery Rev. 2008; 60(15):1638–1649.
37. Bandak S, Ramu A, Barenholz Y, Gabizon A. Reduced Uv-Induced Degradation of Doxorubicin Encapsulated in Polyethyleneglycol-Coated Liposomes. Pharm Res. 1999; 16(6):841–846. [PubMed: 10397603]
38. Lao LL, Peppas NA, Boey FYC, Venkatraman SS. Modeling of Drug Release from Bulk-Degrading Polymers. Int. J. Pharm. (Amsterdam, Neth.). 2011; 418(1):28–41.

39. Lao LL, Venkatraman SS, Peppas NA. Modeling of Drug Release from Biodegradable Polymer Blends. Eur. J. Pharm. Biopharm. 2008; 70(3):796–803. [PubMed: 18577449]

40. Pinto Reis C, Neufeld RJ, Ribeiro AJ, Veiga F. Nanoencapsulation I. Methods for Preparation of Drug-Loaded Polymeric Nanoparticles. Nanomedicine. 2006; 2(1):8–21. [PubMed: 17292111]

41. Williams CG, Malik AN, Kim TK, Manson PN, Elisseeff JH. Variable Cytocompatibility of Six Cell Lines with Photoinitiators Used for Polymerizing Hydrogels and Cell Encapsulation. Biomaterials. 2005; 26(11):1211–1218. [PubMed: 15475050]

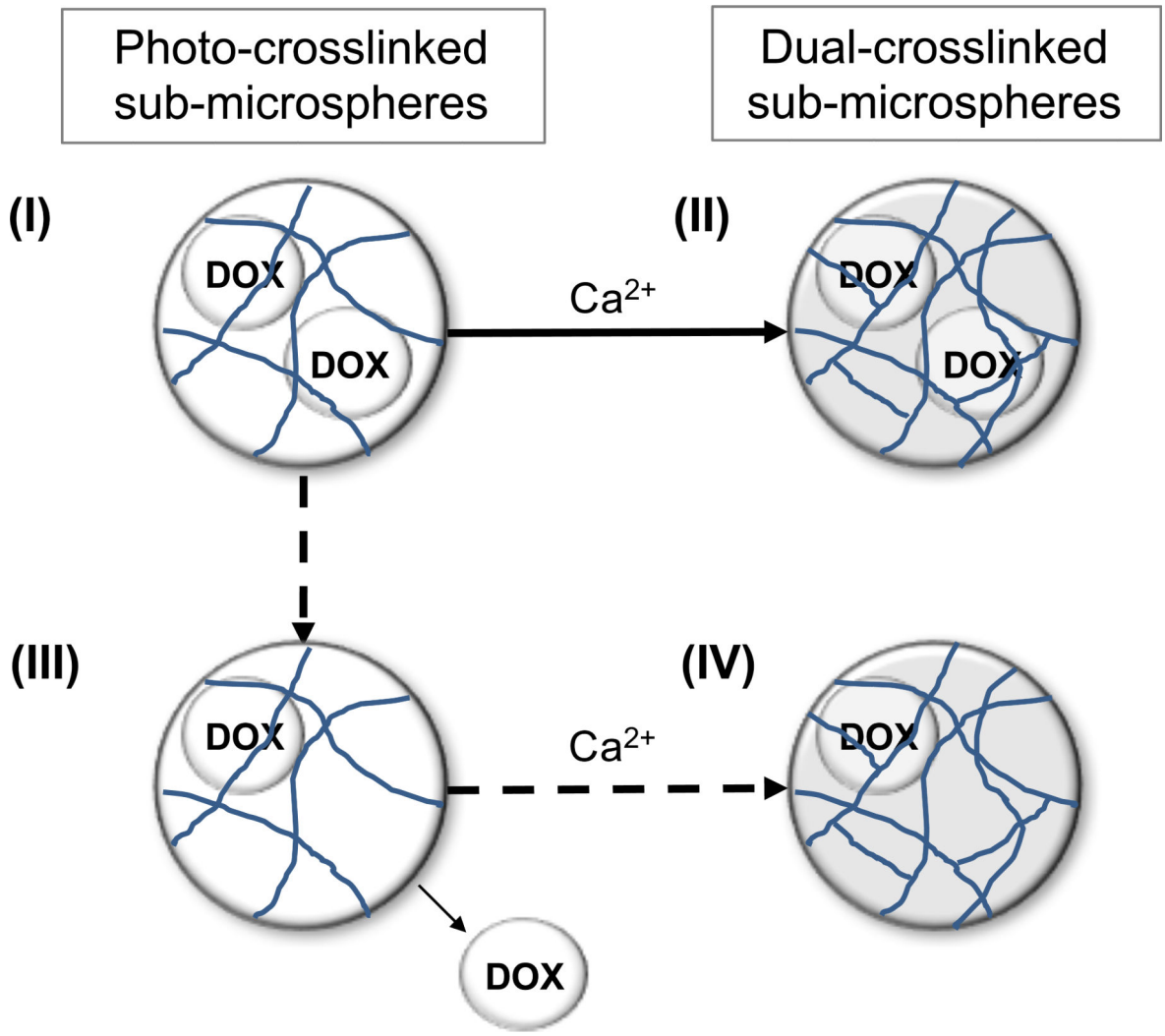

Figure 1.

Schematic of the hydrogel network structure comprising photo-crosslinked and dual-crosslinked Alg-MA sub-microspheres. (I) Photo-crosslinked sub-microspheres exhibit a porous hydrogel network with intermolecular covalent crosslinks, encapsulating DOX. (II) Upon the addition of ionic crosslinking, the hydrogel network tightens, resulting in reduced drug loss and slower diffusion-based drug release; this is the desired product. (III) However, the introduction of aqueous-based calcium chloride ($CaCl_2$) solution may result in drug loss during the ionic crosslinking step. (IV) The non-ideal dual-crosslinked product may exhibit lower drug loading capacity due to the additional steps in the fabrication process.

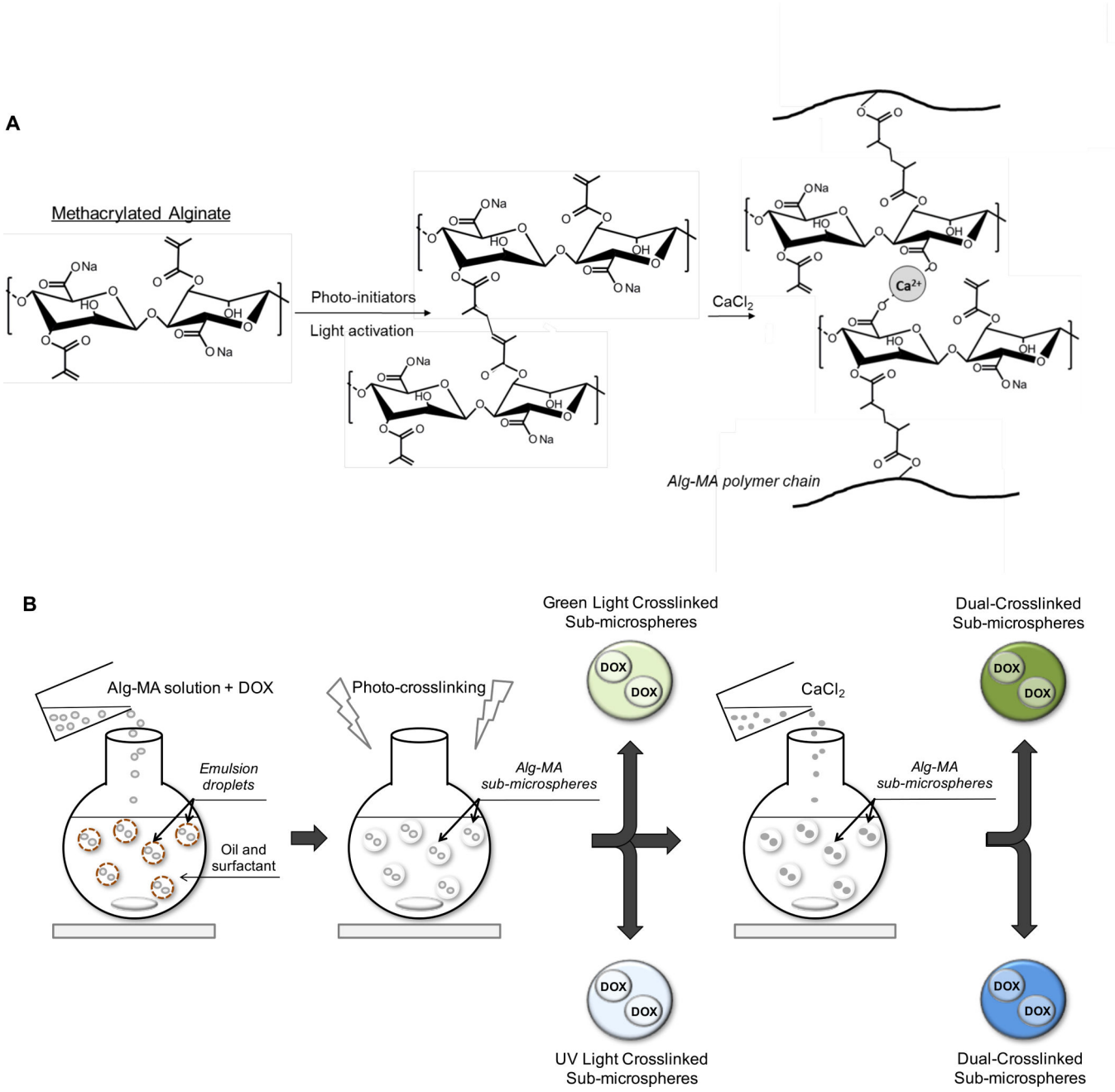

Figure 2.

(A) Chemical structure of methacrylated alginate (Alg-MA). Alg-MA was covalently crosslinked in the presence of photoinitiators under light activation, to form photo-crosslinked Alg-MA hydrogel networks. Alg-MA hydrogels were ionically crosslinked in the presence of calcium chloride ($CaCl_2$) to form dual-crosslinked Alg-MA hydrogel networks. (B) Schematic representation of microsphere fabrication techniques. Microspheres with or without DOX were prepared by premixing Alg-MA solutions and creating a water/oil emulsion at room temperature. Alg-MA sub-microspheres were photo-crosslinked

upon exposure to visible or UV light, respectively, and further dual-crosslinked in the presence of 1 M $CaCl_2$.

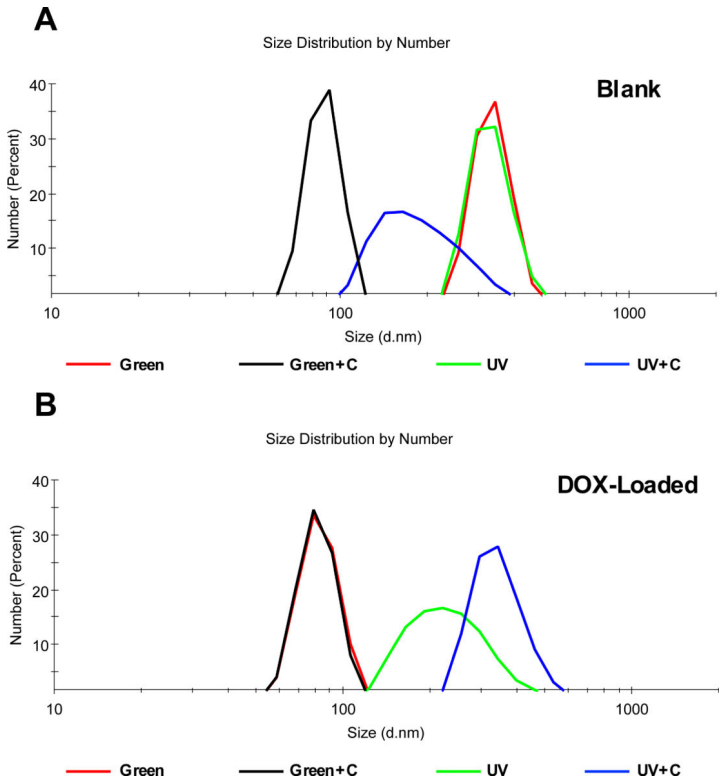

Figure 3.

Dynamic light scattering size distribution plots for photo-crosslinked and dual-crosslinked Alg-MA sub-microspheres both non-loaded/blank (A) and DOX-Loaded (B): green photo-crosslinked (Green), green + Ca^{2+} dual-crosslinked (Green+C), UV photo-crosslinked (UV), UV + Ca^{2+} dual-crosslinked (UV+C). Hydrodynamic diameters were based on number-average calculations.

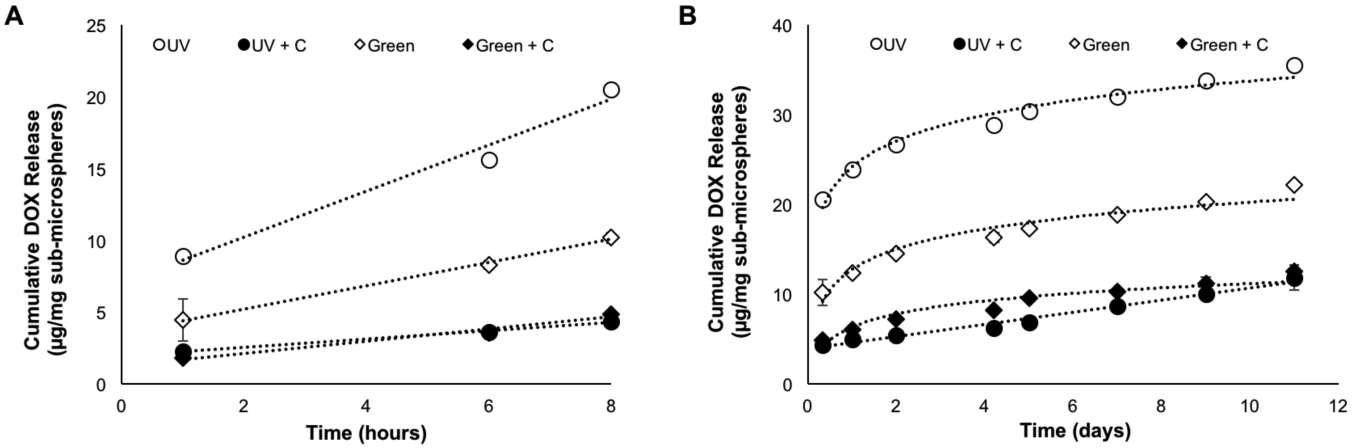

Figure 4.

Quantitative cumulative release of doxorubicin (DOX) from Alg-MA sub-microspheres for 11 days (average ± standard deviation, n = 6 hydrogel samples per group). Various formulations of sub-microspheres were assessed: green photo-crosslinked (Green), green + Ca^{2+} dual-crosslinked (Green+C), UV photo-crosslinked (UV), UV + Ca^{2+} dual-crosslinked (UV+C). Sample aliquots were collected and the DOX concentration was determined using a standard curve at an absorption wavelength of 485 nm. (A) Cumulative DOX release profile during the first 8 hours. (B) Cumulative DOX release profile during 11 days.

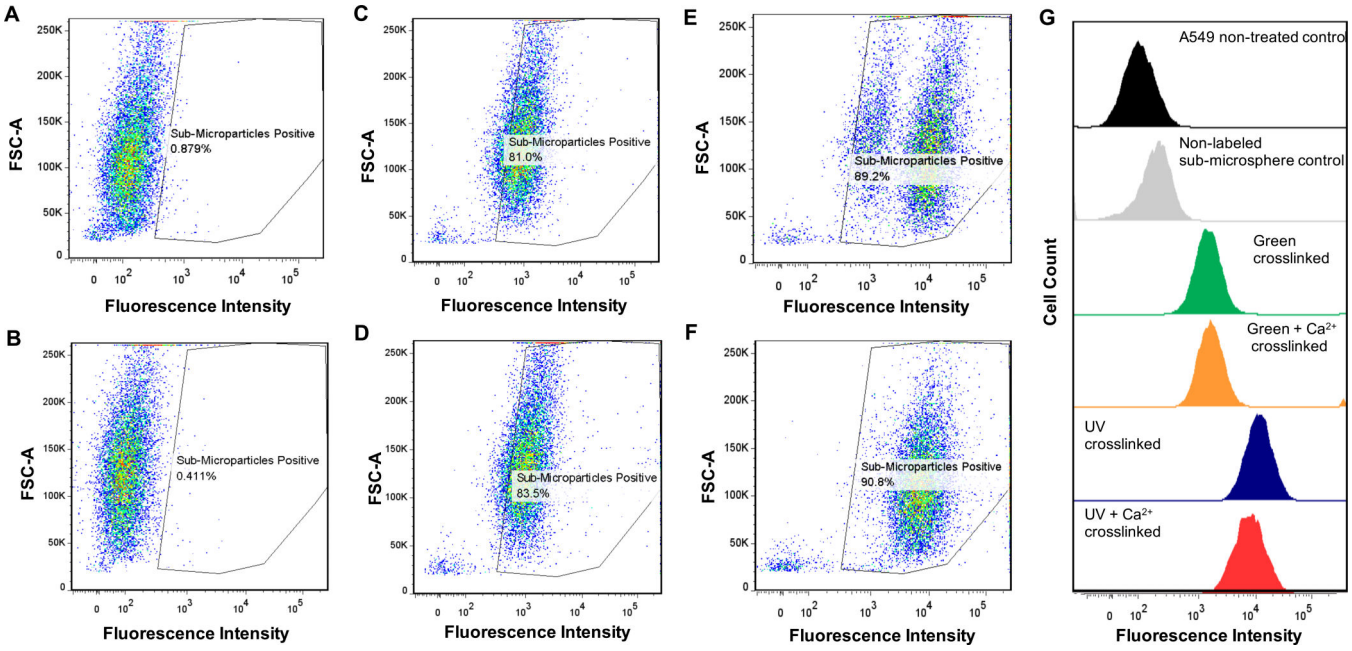

Figure 5.

Flow cytometry analysis of Alg-MA sub-microspheres after 12 hours of co-culture with human lung epithelial carcinoma (A549) cells. (A) Non-treated cell control, (B) cells cultured with non-labeled blank sub-microspheres, (C) cells cultured with green photo-crosslinked sub-microspheres, (D) cells cultured with green photo-crosslinked and calcium crosslinked sub-microspheres, (E) cells cultured with UV photo-crosslinked sub-microspheres, and (F) cells cultured with UV photo-crosslinked and calcium crosslinked sub-microspheres. (G) Flow cytometry histograms were presented to show the different fluorescence intensity between control cells and different Alg-MA sub-microsphere groups.

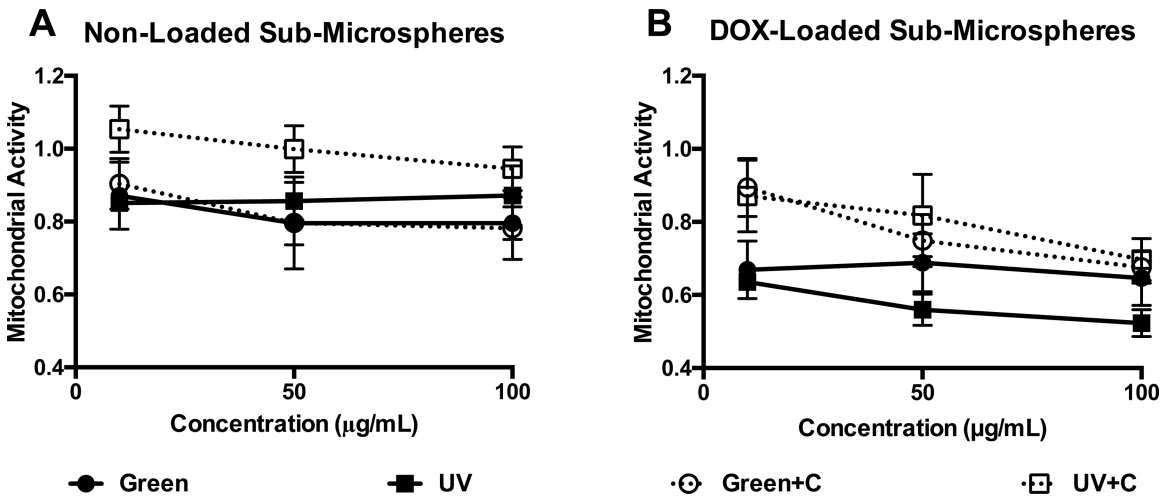

Figure 6.

Human lung epithelial carcinoma (A549) cells were cultured in the presence of hydrogel sub-microspheres for 24 hours in standard growth culture medium at 37°C and 5% CO_2. A549 mitochondrial activity was determined using an absorbance-based quantitative assay; absorbance data for the groups treated with sub-microspheres were normalized to the non-treated cell control (average ± standard deviation, n = 6 hydrogel samples per group). The cytotoxicity of Alg-MA sub-microspheres was analyzed on (A) blank (non-loaded) sub-microspheres. The bioactivity of doxorubicin (DOX) was verified using (B) DOX-loaded sub-microspheres. Various groups (white diamonds = green photo-crosslinked, white circles = UV photo-crosslinked, black diamonds = green + Ca^{2+} dual-crosslinked, black circles = UV + Ca^{2+} dual crosslinked) and sub-microsphere concentrations (10, 50, 100 μg/mL) were characterized.

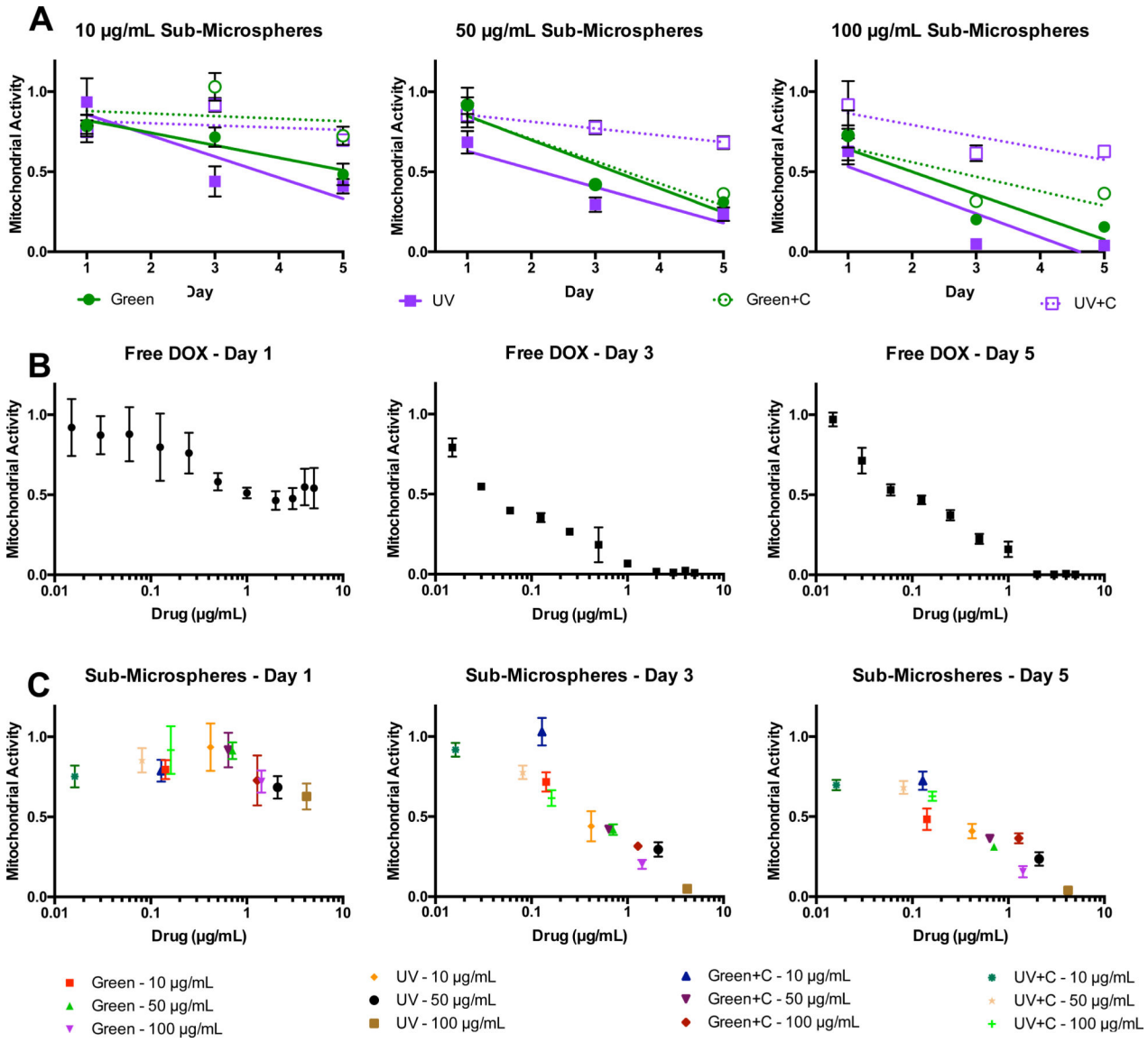

Figure 7.

The efficacy of doxorubicin (DOX)-loaded Alg-MA sub-microspheres as chemotherapeutic delivery vehicles was assessed using a MTT-based assay, to quantify cell proliferation over a 5-day period. A549 activity was recorded as mitochondrial activity and normalized to non-modified cell controls. Various formulations and concentrations (10-100 µg/mL) of sub-microspheres were assessed: green photo-crosslinked (Green), green + Ca^{2+} dual-crosslinked (Green+C), UV photo-crosslinked (UV), UV + Ca^{2+} dual-crosslinked (UV+C). DOX was added exogenously (Free DOX) to the cell culture medium at various concentrations to test the effect of intracellular versus extracellular DOX delivery. (A) Effect of Alg-MA sub-microsphere concentration for each crosslinking type on A549 mitochondrial activity; (B) Effect of ‘free dox’ concentration on A549 mitochondrial activity on days 1, 3, and 5; (C) Effect of DOX concentration encapsulated within Alg-MA sub-microspheres on A549 mitochondrial activity on days 1, 3, and 5.

Table 1

Dynamic light scattering (DLS) quantitative analysis of hydrodynamic diameters and zeta-potentials of blank (i.e., non-loaded) and DOX-loaded photo-crosslinked and dual-crosslinked Alg-MA sub-microspheres. DOX encapsulation efficiencies were determined using an absorbance assay after sub-microsphere fabrication.

Sub-Microsphere Group	Hydrodynamic Diameter by Number (nm)		Zeta-Potential (mV)		Encapsulation Efficiency (%)
	Blank	*DOX Loaded*	*Blank*	*DOX Loaded*	*DOX Loaded*
Green Light	334	391	−37	−27	28
UV Light	331	243	−21	−21	84
Green Light + Calcium	88	358	−29	−33	26
UV Light + Calcium	197	346	−27	−25	3